Rigid-Rod Polyesters with Flexible Side Chains. 4. Thermotropic Behavior and Phase Structures in Polyesters Based on 1,4-Dialkyl Esters of Pyromellitic Acid and 4,4′-Biphenol

Junji Watanabe,* Brian R. Harkness, Masato Sone, and Hideo Ichimura

Department of Polymer Chemistry, Tokyo Institute of Technology, Ookayama, Meguro-ku, Tokyo 152, Japan

*Received July 7, 1993; Revised Manuscript Received October 27, 1993**

ABSTRACT: A series of rigid-rod polyesters with long alkyl side chains, denoted as B-C*n*, have been prepared by condensing 1,4-dialkyl esters of pyromellitic acid with biphenol. The alkyl side-chain lengths were varied from hexyl (n = 6) to octadecyl groups (n = 18), and the thermotropic transition behavior and mesophase structure of these materials were examined by optical microscopy, DSC, and X-ray measurements. An increase in the length of the side chain decreases remarkably the melting point of the crystalline phase, giving rise to a liquid crystalline phase. Two types of liquid crystalline phases with layerlike modifications, LC-1 and LC-2, have been observed. The transition behavior of these liquid crystalline phases is described as a function of the side-chain length. In addition, the structural characteristics of the liquid crystalline phases as well as the crystalline phase are described as based upon X-ray data collected for oriented specimens.

Introduction

There have been several recent reports in the literature concerning the preparation and the physical properties of ridig-rod polymers with long flexible alkyl side chains.[1-16] The most interesting property of these materials is the ability to form layered structures in crystals and liquid crystals when the alkyl side chains reach a critical length. The α-helical poly(γ-alkyl L-glutamates)[1] were the first examples of this type of material, and more recently, aromatic polyesters and polyamides with long alkyl side chains have also been examined.[2-15] The layered phases are characterized by a segregated structure in which the rigid-rod main chains are packed into a layered structure, with the flexible side chains occuping the space between the layers. The formation of the layered structures is therefore due not only to main-chain stiffness but also to the binary molecular structure.

In the first two papers of this series,[14,15] we have described a facile method for preparing rigid-rod aromatic polyesters with long alkyl side chains, from 1,4-dialkyl esters of pyromellitic acid. In this case, the alkyl substituent ranges from hexyl to octadecyl (C6 to C18). Polyesters were prepared by reacting the diacid chloride of the 1,4-dialkyl ester with either hydroquinone or 4,4′-biphenol to generate the series of H-C*n* and B-C*n* polyesters, respectively, where n is the number of carbon atoms in the alkyl side chain. As discussed in a previous report,[15] the H-C*n* polyesters have been observed to form mesophases when the side-chain length is 12–18 carbon atoms. The mesophases were found to adopt a highly ordered layered structure like that reported for other rigid-rod polyesters with long alkyl side chains. On the other hand, the B-C14 polyester as reported in the first paper[14] was observed to form two different types of liquid crystalline layerd structures depending on the temperature. Both of these structures have been found to be different from the layered structure formed by the H-C*n* mesophases.

In this study, we have prepared a series of B-C*n* polyesters in which the alkyl side-chain length ranges from 6 to 18 carbon atoms

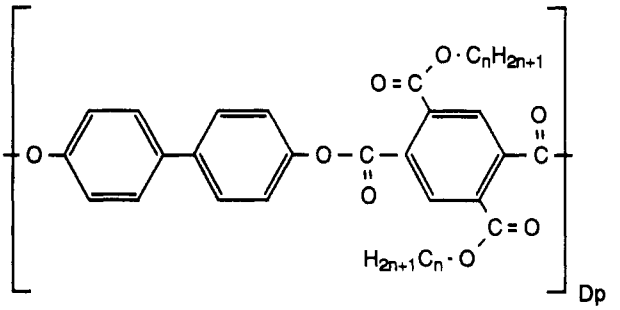

n=6,8,10,12,14,16,18

and analyzed, in detail the thermotropic phase behavior and the mesophase structures. The results will be discussed as a function of side-chain length.

Table 1. Characterization of B-C*n* Polyesters

polymer	inherent viscosity (dL/g)	DSC transition: heating T_1 (°C)	heating T_i (°C)	cooling T_i (°C)	cooling T_2 (°C)	cooling T_1 (°C)
B-C6	0.42	198	233	222		140
B-C8	0.59	61	190	172		40–20
B-C10	0.57	58	160	154		
B-C12	0.71	78	173	168		
B-C14	0.66	124	165	160	103	(−5)[a]
B-C16	0.49	126	131	129	89	(5)[a]
B-C18	0.52	128		117	94	(20)[a]

[a] These transitions may be due to the crystallization of side chains (see the text).

Experimental Section

Materials and Methods. The synthesis and characterization of the 1,4-dialkyl esters of pyromellitic acid have been described in a previous report.[15] The B-C*n* polymers with n = 6–18 were prepared by converting the 1,4-dialkyl esters of pyromellitic acid to their respective diacid chlorides followed by condensation with 4,4′-biphenol. The inherent viscosities of these polymers are listed in the second column of Table 1.

DSC measurements were performed with a Perkin-Elmer DSC II calorimeter at a scanning rate of 10 °C/min. Wide-angle X-ray diffraction patterns of the polymers were recorded with a flat-plate camera mounted to a Rigaku-Denki X-ray generator emitting Ni-Filtered Cu Kα radiation. The temperature of the

* Abstract published in *Advance ACS Abstracts*, December 1, 1993.

0024-9297/94/2227-0507$04.50/0

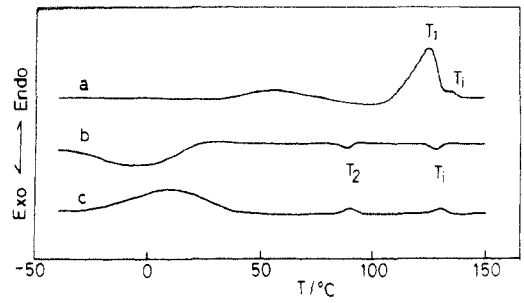

Figure 1. DSC thermograms of the B-C16 cast film observed on (a) first heating, (b) first cooling, and (c) second heating.

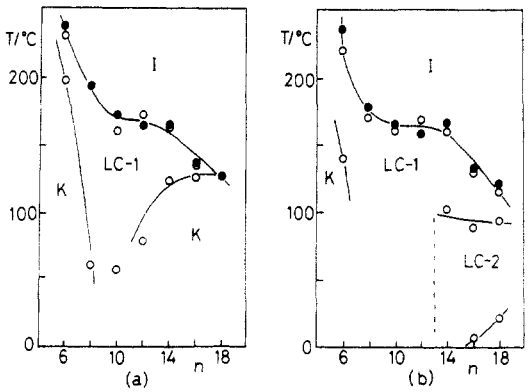

Figure 2. Variation of the transition temperatures with n (the number of carbon atoms in the akyl side chain) as observed on (a) the first heating of as-cast films and (b) cooling. The open circles are based on DSC thermograms, and the closed circles are based on microscopic observations.

samples was controlled by placing them in a Mettler FP-80 hot stage mounted in the beam path. The film to specimen distance was determined by calibration with a silicon powder. Optical microscopic observations of the liquid crystalline texture were made with an Olympus BH-2 polarizing microscope equipped with a Mettler FP-80 hot stage. ^{13}C CP/MAS NMR spectra were measured by means of a JNM-GX270 NMR (67.5 MHz) with a variable-temperature (VT) CP/MAS accessory. The sample (ca. 200 mg) was contained in a cylindrical rotor made of ceramic materials and spun at 4.5–4.8 Hz. The contact time was 2 ms with a repetition time of 5 s.

Results and Discussion

1. Phase Behavior of B-C*n* Polyesters. The B-C*n* polymers were all readily soluble in organic solvents such as THF and chloroform, and from these solutions fine thin films can be prepared by casting. Microscopic observation of these films on heating showed two transitions. At the first transition, T_1, the solid crystalline phase is altered to the fluid liquid crystalline phase, and at the second transition, T_1, the materials enter into the isotropic phase. This transition behavior was also detected by DSC as typically shown for B-C16 in Figure 1. The DSC transition temperatures on heating are listed in the third column of Table 1. The transition temperatures as determined by these two methods roughly correspond to each other although another DSC transition can be observed at around 50 °C for the B–C14, B–C16, and B-C18 polyesters (see curve a of Figure 1). This latter transition may not represent a thermodynamically stable event since it disappears after annealing at 80 °C. The transition temperatures recorded by both methods are plotted against n in Figure 2a, in which the open and closed circles are based on DSC and microscopic measurements, respectively. In this figure, one can observe, on heating, that the isotropization temperatures, T_i, decrease rapidly as n is increased from 6 to 10 but level off for the B-C10, B-C12, and B-C14 polyesters before falling somewhat again for the B-C16 and B-C18 polyesters. Similarly, the melting temperature of the crystal, T_1, decreases but more substantially than T_i when n is increased from 6 to 10. With a further increase of n, T_1 increases again and levels off for B-C14, B-C16, and B-C18. As a result, the liquid crystalline phase appears over a wide temperature range for the B-C*n* polyesters that have an intermediate side-chain length.

The phase behavior observed on cooling is also shown in Figure 2b. The transition temperatures from the isotropic to liquid crystal phase are slightly lower than those observed on heating. An interesting aspect in this case is that the B-C14, B-C16, and B-C18 polyesters show a new second transition (T_2 transition) in the temperature region from 90 to 100 °C (refer to curve b in Figure 1). This can be interpreted as resulting from a transition from one type of liquid crystal to another (i.e., a liquid crystal to liquid crystal transition) as will be described in greater detail later. The DSC cooling scans for the B-C8, B-C10, and B-C12 polyesters are generally featureless, showing only a single phase transition from the isotropic to liquid crystal phase.

The liquid crystal to crystal transition has not been observed for the specimens with the exception of the B-C6 polyester when observed at a normal cooling rate of 10 °C/min. This can be attributed to a greater degree of difficulty in forming crystallites from the longer side-chain derivatives. Therefore, on cooling the B-C8, B-C10, and B-C12 polyesters to room temperature the liquid crystalline phase is retained and frozen. Also for the B-C14 and B-C16, and B-C18 polyesters, the liquid crystalline phase is frozen, but in these cases the side chains can crystallize at temperatures lower than 50 °C (see curves b and c in Figure 1). Reheating and recooling these materials will give phase transitions as shown in Figure 2b.

It should be noted here that these materials when cooled from the isotropic melt can be crystallized by annealing at around 80 °C for an extended period of time, although fairly prolonged annealing for 1 or 2 weeks is necessary for well-developed crystallization to occur. The transition behavior of these annealed materials was found to be virtually identical to those observed for the cast films.

The phase behavior of the polyesters is, therefore, quite sensitive to their thermal history, which can be explained on the basis that kinetic factors lead to slow crystal growth. We can also conclude that all specimens have the ability to form one type of liquid crystal (LC-1) whereas the B-C14, B-C16, and B-C18 polyesters can form an additional liquid crystal (LC-2) in the lower temperature region of LC-1. A comparsion of parts a and b of Figure 2 reveals that the LC-1 is enantiotropic whereas the LC-2 is likely monotropic in nature. The isotropization enthalpy of LC-1 is around 0.15 kcal/(mol of repeat unit) and the enthalpy for the LC-1 to LC-2 transition is about 0.1 kcal/(mol of repeat unit).

2. Crystal Structure of B-C*n* Polyesters. At this point we will focus on the crystal structure of the B-C*n* polyesters. Since the crystal structure obtained for both the as-cast and annealed specimens is virtually identical, the X-ray diffraction pattern has been examined for an oriented crystalline fiber which was spun from the isotropic melt and succeedingly annealed at 80 °C for 2 weeks. Parts a and b of Figure 3 show the oriented crystalline patterns for the B-C6 and B-C18 polyesters, respectively. The diffraction pattern includes a number of layer line reflections as well as equatorial reflections, indicating that the crystal structure has three-dimensional order. The three-dimensional crystal lattice is obviously triclinic; however, a precise determination of the structure has so

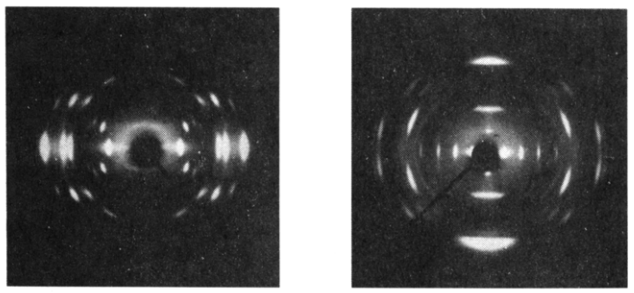

Figure 3. Oriented X-ray patterns of (a) B-C6 and (b) B-C18 crystalline fibers (see the text). Here, the fiber axis is oriented in the vertical direction.

Table 2. X-ray Data for the Equatorial Reflections Observed for B-C6 and B-C18 Fibers

B-C6			B-C18		
d_{obsd} (Å)	$hk0$[a]	d_{calcd}[a] (Å)	d_{obsd} (Å)	$hk0$[a]	d_{calcd}[a] (Å)
9.73 vs	100	9.76	23.1 vs	100	23.0
4.88 s	200	4.88	11.5 s	200	11.5
4.48 s	110	4.43	7.68 m	300	7.68
3.73 vs	210	4.73	5.76 w	400	5.76
2.97 w	310	2.96	4.62 vw	500	4.61
2.36 vw	410	2.38	3.45 m	010	3.45
			3.40 m	110	3.38
			3.27 w	210	3.24
			3.06 vw	310	3.06
			2.87 vw	410	2.87

[a] Indices and d_{calcd} are based on the unit cells cited in the text.

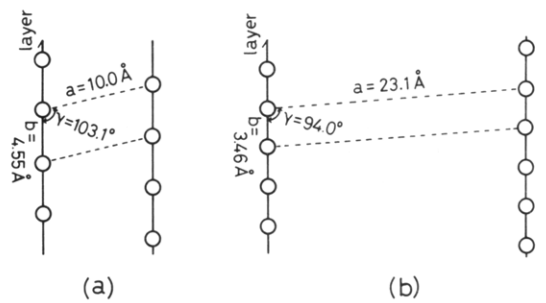

Figure 4. Two-dimensional lattices of (a) B-C6 and (b) B-C18 as elucidated from the equatorial reflections of the oriented X-ray pattern of Figure 3. The open circles in the layers indicate the position of the aromatic main chains.

far not been performed successfully. Hence, we shall refer to the two-dimensional lattice projected along the polymer chain axis, which can be elucidated from the equatorial reflection profiles.

As listed in Table 2, the equatorial reflections include a series of $h00$ reflections. In addition, several other $h10$ reflections are observed. These reflections can allow the unambiguous determination of the two-dimensional lattice structure (this is evident in comparing the observed and calculated spacings in Table 2). The crystal lattices are illustrated in parts a and b of Figure 4, with lattice constants of a = 10.0 Å, b = 4.55 Å, and γ = 103.1° for B-C6 and a = 23.1 Å, b = 3.46 Å, and γ = 94.0° for B-C18, respectively. Within these lattices, it is easy to show that the molecules adopt a layered structure in which the aromatic main chains are packed into a layer with a lateral spacing of b and the side chains occupy the space between layers separated by $a \sin \gamma$. The main chains in the layer assume a fully extended conformation with a repeat length of 16.6 Å that can be elucidated by the height (1/16.6 Å^{-1}) of the first layer line from the equatorial line.

The two-dimensional lattices have also been determined for the other annealed fiber specimens. The layer spacing, $a \sin \gamma$, and the molecular distance within a layer, b, are plotted against n in Figure 5. In this case the data for the B-C10 polyester are not included because of difficulty in obtaining a crystalline sample. An interesting aspect of this figure is that a similar value of around 4.6 Å is observed for the b axis in the shorter side-chain B-Cn polyesters (B-C6, B-C8, and B-C12), whereas the longer side-chain B-C14, B-C16, and B-C18 polyesters exhibit a fairly small value of 3.45 Å. This difference in the lateral packing distance is also reflected in the layer spacing, $a \sin \gamma$, as it varies along the different lines with the side-chain length, n, as found in Figure 5. Thus, the main-chain packing within the layer occurs in a different manner in the two series. This in turn indicates that the main chains must assume different conformations. The structure with the short spacing of 3.45 Å is particularly interesting since this distance corresponds to the van der Waals radius of the phenyl ring, and as a result this requires an unusual main-chain conformation, with the aromatic rings forced to have a coplanar arrangement.[17] In fact, recent studies by solid-state ^{13}C NMR and Raman spectroscopies support such a peculiar conformation, the results of which will be reported elsewhere.[16,18]

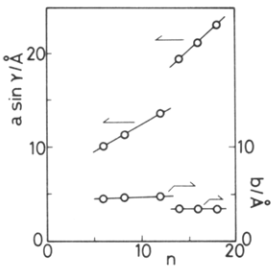

Figure 5. Variation of $a \sin \gamma$ and b (in the two-dimensional lattices) as a function of n (refer to Figure 4).

Table 3. ^{13}C NMR Chemical Shifts for the Aliphatic Carbons of the B-C18 Polyester at Various Temperatures

	^{13}C NMR chemical shift (ppm)						
			interior CH_2*				
temp (°C)	OCH_2	β	C	A	δ	α	CH_3
25	67.1	35.9	34.2	30.8	28.7	24.5	16.1
90	67.0	32.7		30.5	26.7	23.4	14.6
148	67.0	32.3		30.1	25.5	23.0	14.3

[a] C and A indicate the crystalline and noncrystalline states, respectively.

The side chains located in the space between the main-chain layers are also essentially in a crystalline form, which can be examined by solid-state ^{13}C NMR spectroscopy. Figure 6 shows the spectra for the B-C18 crystal as observed in the range of 0–80 ppm, the signals of which can be assigned to the carbons of the akyl side chain. The spectra of the LC-2 and isotropic phases are also shown in the same figure. The values of the chemical shifts for the peaks together with their assignment are listed in Table 3. The peaks in the vicinity of 30 ppm can be assigned to the interior CH_2 carbons and have been used to discuss the conformation and/or crystal structure of the alkyl chains.[19,20] From reference data on n-alkanes and polyethylene,[21] peak C at 34.2 ppm arises from the CH_2 carbons in an all-trans zigzag conformation in the crystalline phase and peak A at 30.1 ppm arises from the carbons in a noncrystalline state. The crystalline phase of B-C18, obviously, shows an intense peak C and small peak A, indicating some parts of side chain are in a noncrystalline state. In contrast, the liquid crystalline and isotropic phases show only a peak A, indicating that they include only noncrystalline side chains.

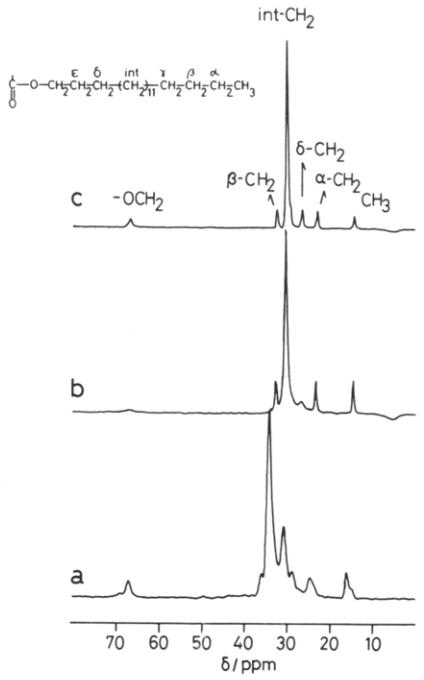

Figure 6. ^{13}C CP/MAS NMR spectra recorded for the aliphatic side chains of the B-C18 polyester: (a) crystalline phase at 20 °C; (b) LC-2 phase at 90 °C; (c) isotropic phase at 150 °C.

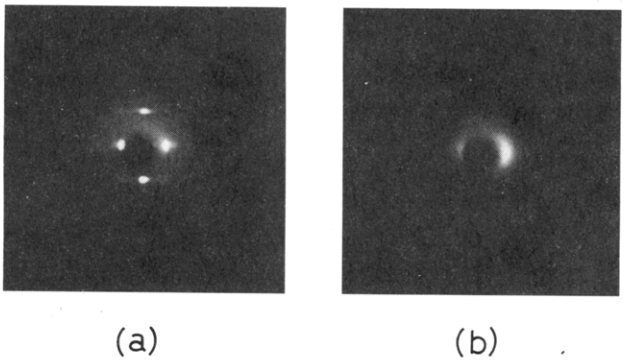

Figure 7. Oriented X-ray patterns of (a) the LC-2 phase and (b) the LC-1 phase of the B-C18 polyester.

3. Structure of Liquid Crystal-2 (LC-2) Phase. LC-2 is a monotropic liquid crystal and appears on cooling the B-C14, B-C16, and B-C18 polyesters (refer to Figure 2b). The viscosity of this phase is fairly high and so no characteristic optical texture can be detected. The X-ray diffraction pattern for the oriented LC-2 phase of B-C18 is shown in Figure 7a. The pattern includes several characteristic sharp reflections although the number of reflections have been reduced to a great extent as compared to the crystal diffraction pattern of Figure 3b. In the small-angle region, two sharp equatorial reflections indexed by 100 and 200 are observed with spacings of 25.0 and 12.4 Å, respectively. In addition, two sharp meridional reflections with spacings of 16.6 (001) and 8.30 Å (002) are also observed. The weak 101 reflection also appears with a spacing of 13.9 Å. In the wide-angle region, broad arcs with a spacing of 4.5 Å can be observed. This diffraction pattern is also typical of the LC-2 phase formed by B-C14 and B-C16. The X-ray data are listed in Table 4, and the spacings of the 100 reflections are plotted as closed circles against n in Figure 8.

It should be noticed that the spacing of the equatorial reflection approximates to that of the crystalline phase, indicating that the mesophase also assumes a layered structure. A 16.6-Å meridional reflection reveals that the main chains still assume a fully extended conformation as in the crystalline phase. The intensity of this reflection as well as the appearance of the second-order reflection indicates that there is a positional order along the chain axis in each layer. From the observation of the 101 reflection, the positional order may be more or less correlated between adjacent layers. The lack of a 010 reflection is characteristic of this mesophase and indicates that there is disorder in the lateral packing of the main chains. The ^{13}C NMR spectra as mentioned above dictate that the side chains located between the layers must be disordered. These two latter facts as well as the fluidity of this phase undoubtedly differentiate this layered phase from the layered crystalline phase and give its liquid crystalline nature. An illustration of the layered structure in this mesophase is given in Figure 9.

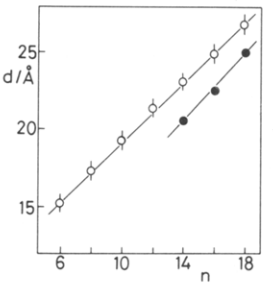

Figure 8. Plots of the spacings of the 100 reflections for LC-2 and LC-1 against n. Here, the closed circles are observed for the LC-2 phases, while the open circles are observed for the LC-1 phases.

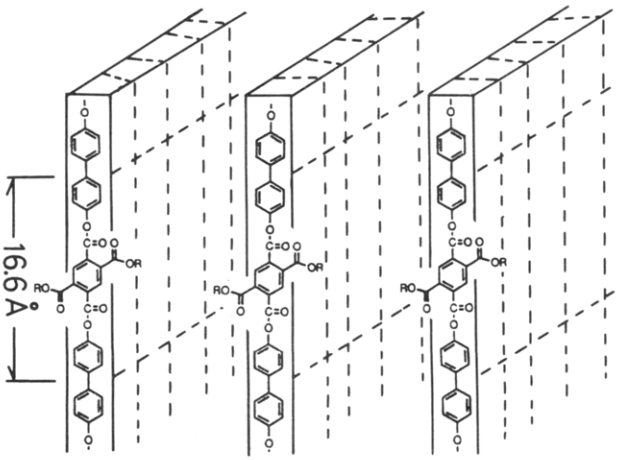

Figure 9. Schematic illustration of the layerd structure for the LC-2 phase. Here, the fully extended main chains are packed into a layer with only a positional order along their chain axes, and the side chains in the melt occupy the space between the layers.

Table 4. X-ray Data for the LC-2 Phases

d_{obsd} (Å)		
B-C14	B-C16	B-C18
20.5 (100)	22.7 (100)	25.0 (100)
16.6 (001)	16.6 (001)	16.6 (001)
12.9 (101)	13.6 (101)	13.9 (101)
10.2 (200)	11.3 (200)	12.4 (200)
8.30 (002)	8.31 (002)	8.30 (002)

4. Structure of Liquid Crystal-1 (LC-1) Phase. LC-1 has been observed to occur in all specimens. The X-ray pattern for the oriented LC-1 mesophase of B-C18 is shown in Figure 7b. Compared to the lower temperature LC-2 mesophase, the X-ray pattern for this mesophase is greatly simplified and exhibits only a few broad reflections. In the small-angle region, one broad equatorial reflection with a spacing of 27 Å is observed. A very weak meridional arc with a spacing of 15.5 Å is also observed. In the wide-

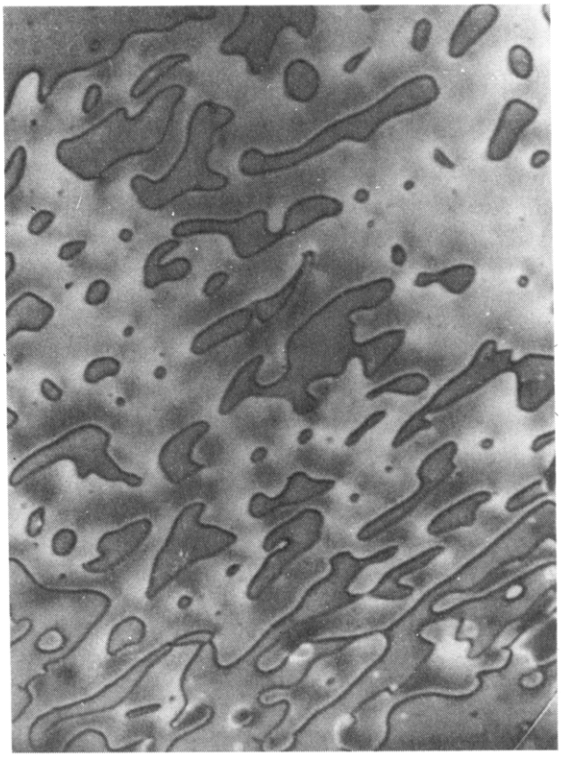

Figure 10. Optical microscopic photograph for the LC-1 phase of B-C10 exhibiting an inversion wall texture.

angle region, only a broad arc with a spacing of approximately 4.5 Å can be distinguished. This mesophase, thus, has no long-range translational order, which is a characteristic feature of nematic mesophases. A similar pattern is observed for the LC-1 phases of the other B-C*n* polyesters. In Figure 8, the spacings of the equatorial reflections are plotted as open circles against *n*, as measured for the mesophases at 100 °C. The spacing of the equatorial reflection increases monotonically from 15 to 27 Å when the value of *n* increases from 6 to 18, whereas the spacing of the meridional arc is almost constant at around 15.5 Å.

By optical microscopy, it was oberved that this phase exhibits fluid behavior between glass slides and has an inversion wall texture like that of a nematic phase (see Figure 10). In areas where there is a free surface on one side, a Schlieren texture can also be observed. A similar texture has been observed for similar types of polyesters prepared by Ballauff et al.[4] The fluidity and microscopic Schlieren texture, thus, undoubtedly reflect the nematiclike character of the mesophase.

In this case, however, the X-ray data do not support the conclusion that this is an ordinary nematic phase. The reason for this is that the spacing of the equatorial reflection is too large to accommodate the molecules in a nematic field. In an ordinary nematic phase, each molecule functions independently as a kinetic unit and therefore rotates freely around the long axis. If such is to occur in this system, spacings less than 10 Å are expected since the spacing should correspond to the average diameter of molecule. As found in Figure 8, however, the observed spacing of the equatorial reflection is as large as that observed for the LC-2 phase. A similar phenomenon has been observed for the nematic phases of polyamides with alkyl side chains as reported by Ebert et al.[8,9]

To explain this curiosity, two possible nematic structures can be proposed as illustrated in parts a and b of Figure 11. One of these has been proposed for the polyamides, by Ebert et al.,[8] in which each molecule functions as a kinetic unit but retains a boardlike shape as in the layered

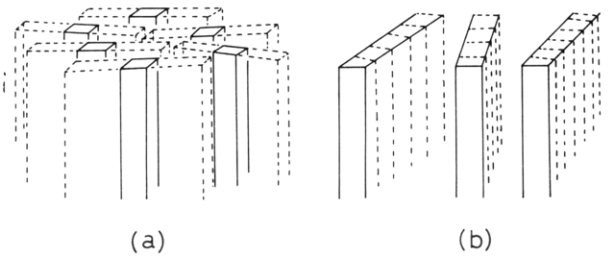

Figure 11. Two possible nematic structures for the LC-1 phase. In the nematic phase of a, the molecules having a broadlike shape function as a kinetic unit. In contrast, in the nematic phase of b, the main chains are associated with each other to form a layer, but the layers are piled up with a greater degree of disorder.

LC-2 (see Figure 11a). To retain such a boardlike shape, the polymer main chains should be coplanar and also the flexible side chains should have a strong tendency to remain within the planes defined by the backbone. For these polyesters, such a peculiar conformation appears unlikely in the nematic field since no specific intermolecular interactions can be expected.[17] As a more plausible model, it can be speculated that the main chains are still associated with each other to form a layer but the layers are piled up with a greater degree of disorder (see Figure 11b). To produce such a disorder, the layer may be constructed with only short-range order. We do not yet have decisive evidence as a basis for selecting one of the two possible structures.

Finally, it is noteworthy that both of the proposed nematic phases should be biaxial. In fact, the biaxiality has been observed in the above-mentioned nematic phase of polyamides as detected by the conoscopic method.[9]

Concluding Remarks

To conclude, the B-C*n* polyesters form layered crystalline and liquid crystalline phases in which the aromatic main chains are packed into a layer and the alkyl side chains are located in the space between the layers.

In the crystalline phase, the aromatic main chains are in a fully extended form with a repeating length of 16.6 Å and these are regularly packed within a layered structure. In addition, the side chains are also in a crystalline state between the layers. The X-ray pattern is indicative of a crystal structure with three-dimensional order, which demands that the positional correlation between adjacent layers is maintained through the side-chain crystals. Thus, the crystal structure is likely built up by a close coupling of main-chain crystals and side-chain crystals. This coupling is also supported by the fact that both crystals melt at the same temperature. A study is now in progress to more accurately determine the structure of the three-dimensional crystal lattice.

It is interesting to note that the main chains are packed into two different layered structures depending on the side-chain length. For the B-C*n* polyesters with side chains shorter than $n = 12$, the lateral packing distance of the main chains within a layer is 4.6 Å, but this reduces to 3.45 Å for the B-C*n* polyesters with side chains longer than $n = 14$ (see Figure 4). The packing distance of 4.6 Å in the former group is reasonable for the main chains which have the twisted conformation in the most stable energy.[11,17] In contrast, the short spacing of 3.45 Å in the latter group indicates the anomalously close packing of main chains and requires a peculiar conformation in which the phenyl rings adopt a coplanar arrangement.

A difference in the packing structure between the two groups is also reflected in the melting temperature of the crystals. As shown in Figure 2a, the melting temperature drops significantly with an increase of *n* from 6 to 10 but

then increases again with a further increase of n. The two distinct regions identified in the phase diagram are obviously related to the crystal structures. The decreasing region, observed for the short side-chain B-Cn, corresponds to the lowering of the thermal stability of the crystal structure, which is determined mainly by the polymer backbones with perhaps a slight perturbation by the shorter side chains. On the other hand, the regime of increasing thermal stability, observed with the longer alkyl side-chain polyesters, corresponds to an enhancement of the thermal stability of the crystals. The structure in this case is strongly dominated by the crystallization of the long paraffin side chains, which also likely results in the anomalously dense packing of the backbones within a layer as described above.

LC-2, the lower temperature mesophase, also has a layered segregated structure similar to that of the crystalline phase although its fundamental structure is remarkably altered in several aspects from the crystal structure. The main chains are still in an elongated conformation (a repeat length of 16.6 Å) as in the crystalline phase, but they are packed into a layer having positional order only along the chain axis but not in the lateral direction. The side chains are included between the layers in a noncrystalline form, which gives rise to the liquid crystalline fluidity of the phase. It is interesting to note that this type of liquid crystalline phase appears only for the B-Cn polyesters in which the alkyl side-chains are longer than n = 14. The length of the side chains, hence, is a significant factor for determining the nature of the liquid crystalline phase.

This layered LC-2 has interesting features compared to the layered LC observed for the H-Cn polyesters. In the latter, the main chains pack into a layer with positional order in the lateral direction but not along the chain axis.[15] This is opposite to that in the LC-2 of B-Cn. Furthermore, Ballauff et al.[4] have reported in the layered mesophases formed by the polyesters

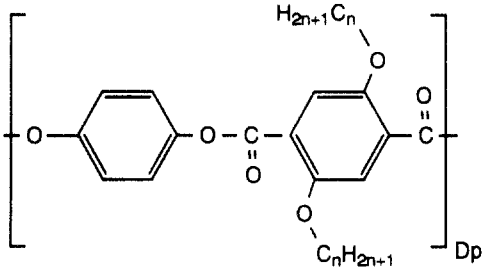

no positional order can be seen in any direction so far as the main-chain packing within a layer is concerned. These observations suggest that there are several types of layerd mesophases which have different modes of packing the main chains into a layered structure as described below.

The LC-1 observed for all specimens displays a nematiclike optical texture, but a classical nematic phase cannot be postulated because of the large lateral packing spacing between the molecules. At the present time, we can only propose a tentative model in which the molecules retain a layerlike structure but there are frequent irregularities in the packing. A more detailed examination is needed for clarification of the structure.

Finally, it is interesting to note that the basic features of the molecular packing into a layered mesophase are similar to those of discotic columnar phases.[22,23] In columnar phases, the column is formed by a stacking of the disklike molecules with the long alkyl side chains and core molecules arranged in space with a two-dimensional lattice structure that may be hexagonal or rectangular. The different types of columnar phases have been classified on the basis of the packing array of the disklike molecules into a column and the two-dimensional packing array of columns.[22] In the present layered mesophase, the molecules have a boardlike shape and associate into a layered structure. In analogy to the discotic phases, the layered mesophases can be classified into several types on the basis of the packing arrangement of molecules into a layer.[24] This classification was initially proposed by Ebert et al.,[9] who termed the layered mesophases "sanidic" and defined by Greek letter Σ. We are in agreement with this terminology, which can be extended to account for the four possible types of sanidic mesophases, Σo_b, $\Sigma o_{u\perp}$, $\Sigma o_{u\parallel}$, and Σd. These have the following packing characteristics of the main chains within a layer:

1. Σo_b: having positional order in both directions parallel and perpendicular to the chain axis.
2. $\Sigma o_{u\perp}$: having positional order only in a direction perpendicular to the chain axis.
3. $\Sigma o_{u\parallel}$: having positional order only in a direction parallel to the chain direction.
4. Σd: having no positional order in any direction.

According to this classification scheme, the LC-2 in the present B-Cn polyesters belongs to $\Sigma o_{u\parallel}$ while the layered mesophase of H-Cn belongs to $\Sigma o_{u\perp}$. Further, the layered mesophase reported by Ballauff et al.[4] can be classified into Σd. The appropriateness of this classification scheme may be clarified after a detailed structural examination of many types of layered mesophases.

References and Notes

(1) Watanabe, J.; Ono, H.; Uematsu, I.; Abe, A. *Macromolecules* **1985**, *18*, 2141.
(2) Ballauff, M. *Makromol. Chem., Rapid. Commun.* **1986**, *7*, 407.
(3) Ballauff, M. *Angew. Chem., Int. Ed. Engl.* **1989**, *28*, 253.
(4) Ballauff, M.; Schmidt, G. F. *Mol. Cryst. Liq. Cryst.* **1987**, *147*, 163.
(5) Stern, R.; Ballauff, M.; Wegner, G. *Makromol. Chem., Makromol. Symp.* **1989**, *23*, 373.
(6) Galda, P.; Kistner, D.; Martin, A.; Ballauff, M. *Macromolecules* **1993**, *26*, 1595.
(7) Rodrigues-Parada, J. M.; Duran, R.; Wegner, G. *Macromolecules* **1989**, *22*, 2507.
(8) Ebert, M.; Herrmann-Schenherr, O.; Wendorf, J. H.; Ringsdorf, H.; Tschirner, P. *Makromol. Chem., Rapid Commun.* **1988**, *9*, 451.
(9) Ebert, M.; Herrmann-Schenherr, O.; Wendorf, J. H.; Ringsdorff, H.; Tschirner, P. *Liq. Cryst.* **1990**, *7*, 63.
(10) Stern, R.; Ballauff, M.; Lieser, G.; Wegner, G. *Polymer* **1991**, *32*, 2096.
(11) Adam, A.; Spiess, H. W. *Makromol. Chem., Rapid Commun.* **1990**, *11*, 249.
(12) Baldwin Frech, C.; Adam, A.; Falk, U.; Boeffel, C.; Spiess, H. W. *New Polym. Mater.* **1990**, *2*, 267.
(13) Clauss, J.; Schmidt-Rohr, K.; Adam, A.; Boeffel, C.; Spiess, H. W. *Macromolecules* **1992**, *25*, 5208.
(14) Harkness, B. R.; Watanabe, J. *Macromolecules* **1991**, *24*, 6759.
(15) Watanabe, J.; Harkness, B. R.; Sone, M. *Polym. J.* **1992**, *24*, 1119.
(16) Sone, M.; Harkness, B. R.; Watanabe, J.; Torii, T.; Yamashita, T.; Horie, K. *Polym. J.* **1993**, *25*, 997.
(17) Hummel, J. P.; Flory, P. J. *Macromolecules* **1980**, *13*, 479.
(18) Sone, M.; Harkness, B. R.; Watanabe, J.; Kurosu, H.; Ando, I., to be published.
(19) Yamanobe, T.; Tsukahara, M.; Komoto, T.; Watanabe, J.; Ando, I.; Uematsu, I.; Deguchi, K.; Fujito, T.; Imanari, M. *Macromolecules* **1988**, *21*, 48.
(20) VanderHart, D. L. *J. Magn. Reson.* **1981**, *44*, 117.
(21) Earl, W. L.; VanderHart, D. L. *Macromolecules* **1979**, *12*, 762.
(22) Destrade, C.; Foucher, P.; Gasparoux, H.; Tinh, N. H.; Levelut, A. M.; Malthete, J. *Mol. Cryst. Liq. Cryst.* **1981**, *71*, 111.
(23) Chandrasekhar, S.; Ranganath, G. S. *Rep. Prog. Phys.* **1990**, *53*, 57.
(24) In columnar phases, the columns associate with two-dimensional positional order, but in this case the layers are piled up with one-dimensional order. Hence, in our classification of the layered structures we do not consider the difference in the packing of layers but only the difference in the main-chain packing into a layer.